Three-body continuum states and Efimov physics in noninteger geometry

E. Garrido [1] E. R. Christensen [2] and A. S. Jensen[2]

[1]*Instituto de Estructura de la Materia, IEM-CSIC, Serrano 123, E-28006 Madrid, Spain*
[2]*Department of Physics and Astronomy, Aarhus University, DK-8000 Aarhus C, Denmark*

Continuum structures of three short-range interacting particles in a deformed external one-body field are investigated. We use the equivalent d method employing noninteger dimension, d, in a spherical calculation with a dimension-dependent angular momentum barrier. We focus on dimensions close to the critical dimension, $d = d_E$, between 2 and 3, defined by zero two-body energies, where the Efimov effect can occur. We design for this dimension region a schematic, long-distance realistic, square-well based, three-body spherical model, which is used to derive analytic expressions for the wave functions, scattering lengths, phase shifts, and elastic-scattering cross sections. The procedure and the results are universal, valid for all short-range potentials, and for large scattering lengths. We discuss the properties and validity of the derived expressions by means of the simplest system of three identical bosons. The derived expressions are particularly useful for very small energies, where full numerical calculations are often not feasible. For energies where the numerical calculations can be performed, a good agreement with the analytic results is found. These model results may be tested by scattering experiments for three particles in an equivalent external deformed oscillator potential. The cross sections all vanish in the zero-energy limit for $d < 3$ with definite d-dependent power of energy.

I. INTRODUCTION

Different spatial dimensions are known to exhibit very different few-body structures as exemplified by the Efimov effect [1–6], which is present in three but absent in two dimensions [7]. This fact implies that some states must change character from bound to continuum states, or vice versa, when the spatial dimension varies continuously between 2 and 3. An analytic continuation connecting these two dimensions is therefore interesting. This is testified by previous investigations using methods designed to reveal the huge variation of the properties [8–12].

The continuous dimension, d, is directly a parameter in the spherical d method introduced in Ref. [7]. The corresponding theoretical description of noninteger dimension connecting these limits has been developed during the last years for two and three bound particles [13–16]. The method is technically precisely as complicated as other few-body calculations without any external field. The simplification is achieved by use of a centrifugal dimension-dependent barrier, which replaces, and is equivalent to use of, a deformed external squeezing potential in ordinary three-dimensional calculations. One significant achievement from this method was the demonstration that the Efimov effect can be induced by an external squeezing potential acting in three dimensions [16], which corresponds to a critical dimension, $d = d_E$, in the d formalism.

The d method has so far only been applied to bound states, which, by definition, fall off exponentially with increasing relative distance. However, very recently the method has been extended to two-body continuum states, where wave functions, scattering lengths, phase shifts, and cross sections are computed [17]. This extension is far from trivial, since the wave functions now extend their oscillations to infinity in the nonconfined directions. Furthermore, phase shifts in the spherical d method involve finite, and in general noninteger, effective angular momentum, where the realizable deformed external field has no angular momentum barrier. It is then remarkable that the d-method phase shift is equal to the phase difference between the two equivalent three-dimensional two-body wave functions calculated with and without short-range interaction [17].

The actual interest in the present type of d-method investigations is that practical up-to-date few-body calculations for cold atomic and molecular gases are easily possible. The measurements on such gases involve simulation and manipulation in laboratories. These experimental methods are extremely flexible, allowing both huge two-body interaction variation as well as an overall confining deformed external field [18–24]. In strong contrast to many-body approximations [25], the advantage of few-body physics is that all degrees of freedom are accurately treated. Two-body theoretical physics is close to being analytic and even universal in the large-distance limit for short-range interactions. The universality can be used to compare properties of systems from different subfields and therefore a tool to exchange knowledge between science subfields [1,6,7,26–31].

However, the necessary external field on two interacting particles increases the difficulties to the nonanalytic level of a three-body problem. This is accentuated if one particle is added to a total of three particles, which in an external field would be equivalent to a four-body problem. The

computational simplification of reducing the number of degrees of freedom as offered by the d method is tempting. However, the d method applied to three particles is only available for bound states, but not established for continuum properties. Thus, so far scattering experiments cannot be analyzed.

The purpose of the present paper is to repair this deficiency and report on the extension of the d method to three particles in the continuum, that is, wave functions, scattering lengths, phase shifts, and cross sections. Scattering, or continuum structure, is more difficult to treat than discrete bound-state properties [32,33]. Three particles may reveal new possibilities as seen for Efimov induced bound states [16]. In fact, we shall in particular focus on dimensions close to the critical value, d_E, where the Efimov conditions are close to being fulfilled. In this region, for $d \lesssim d_E$, the energy of the bound two-body subsystems is very small, making it pretty difficult to compute numerically the elastic phase shifts of the so-called $1 + 2 \rightarrow 1 + 2$ reactions, corresponding to an elastic collision between a particle and a bound two-body system, for collision energies below the two-body breakup threshold. In this case the energy window available for the projectile is extremely small, and the correct asymptotics of the wave function is reached at an extremely large distance, where the three-body wave function should be computed with sufficient accuracy [34–37]. Analytic expressions for these phase shifts, as well as for the case of $3 \rightarrow 3$ reactions, with pure initial and final three-body states, will be provided.

These three-body systems may themselves be of practical use, but also able to teach us how to create and control similar properties in systems, which so far are outside experimental reach. The paper is organized into the introduction in Sec. I followed by Sec. II, presenting the formalism and describing a semirealistic model providing analytic expressions for scattering length and phase shift. The properties of the three-body potentials and the phase shifts are discussed and illustrated in Sec. III. The connection between the computed d-dimensional wave function and the one corresponding to the squeezed three-dimensional space, which allows one to compute observables like the cross section, is discussed in Sec. IV. Finally, Sec. V contains the summary and the conclusions.

II. THREE-BODY CONTINUUM STATES

The basic method to treat three-body systems relies on the use of hyperspherical coordinates, where several bound-state investigations are available in the literature for noninteger dimensions [13–15]. The hyper-radius, ρ, is defined by

$$mM\rho^2 = \sum_{i<j} m_i m_j (\mathbf{r}_i - \mathbf{r}_j)^2 \qquad (1)$$

in terms of the radii, $\mathbf{r}_i$, and masses, m_i, of the three particles, $M = m_1 + m_2 + m_3$, and m is the arbitrary normalization mass.

Interesting structures are related to changing dimensions, as already seen for two particles. However, the pathological Efimov effect for three particles is producing numbers of bound states varying from zero at $d = 3$ over infinitely many at $d = d_E$, and back again to a finite number for $d = 2$. The strong variation of numbers and energies of bound states and

resonances must necessarily influence cross sections for various types of scattering between three particles. Investigating the corresponding d-dependent properties of these states is the purpose of this section, where we use an appropriate semirealistic schematic large-distance model to extract the essence. For simplicity, we shall consider a three-body system where only relative s waves enter.

A. Semirealistic model

We seek analytic insight, which only can be obtained by use of schematic models, where approximations are inevitable. When applied to few-body systems, and in particular to three-body systems, this kind of model, despite its simplicity, permits a simple access to their main properties and characteristics, which furthermore are often described with sufficient accuracy [38]. We shall focus on structures arising when the Efimov conditions are approached, i.e., for values of d in the vicinity of the critical dimension d_E. In this context, we shall first derive three-particle scattering properties.

The key equation is the decoupled reduced radial, ρ-dependent, s-wave Schrödinger equation, that is, [7,15]

$$\left(-\frac{\partial^2}{\partial \rho^2} + \frac{\lambda(\rho) + \ell_d(\ell_d + 1)}{\rho^2} - \frac{2m}{\hbar^2} E \right) f(\rho) = 0, \qquad (2)$$

where $\ell_d = d - 3/2$ is the d-dependent effective angular momentum quantum number for three particles. We immediately emphasize that the $\ell_d \equiv \ell_{d,N=3}$ used in Eq. (2) for three particles differs from $\ell_{d,N=2} = (d - 3)/2$ for two particles. This use of noninteger angular momentum quantum number is similar to the Regge pole analytic continuation [39].

The hyperangular eigenvalue, $\lambda(\rho)$, includes the short-range interaction; it is in principle ρ dependent, and it is in general fully determined for all ρ, from zero to infinity, in the d-dependent adiabatic hyperspherical expansion method [7]. We emphasize that we consider only the lowest adiabatic potential, assumed to be decoupled from the rest. This assumption is pertinent when describing low-energy phenomena, such as the Efimov physics. In fact, in the limit of zero energy and infinite scattering lengths, the nonadiabatic coupling terms are identically zero.

We note that Eq. (2) defines a reduced radial equation with an effective potential:

$$U_{\text{eff}} = \frac{2m}{\hbar^2} V_{\text{eff}} = \frac{\lambda(\rho) + \ell_d(\ell_d + 1)}{\rho^2}. \qquad (3)$$

The details of the short-range three-body potential are unimportant in the cases of our interest, where the large-distance properties are decisive. This has two consequences. First, the only role played by the short-distance $\lambda(\rho)$ behavior is to deliver the attraction required for the three-body system. We are free to use any schematic three-body potential for small ρ, for example a square-well or its limit of a zero-range potential. Second, for our purpose we can efficiently use the universal large-distance structure for $\lambda(\rho)$. Thus, we divide the ρ axis into three intervals: $0 \leqslant \rho \leqslant \rho_0$ (interval I), $\rho_0 \leqslant \rho \leqslant |a_{\text{av}}|$ (interval II), and $\rho \geqslant |a_{\text{av}}|$ (interval III). The two separating lengths, ρ_0 and $|a_{\text{av}}|$, will be defined in the following discussion.

The small-distance interval, $0 \leqslant \rho \leqslant \rho_0$, interval I, contains the dependence on the small-distance properties of the two-body potentials involved in the three-body system, the main effect of which is to determine the energy of the bound three-body state, upon which the possible series of excited, possibly Efimov, states are built. The structures of these excited states are potential independent in the sense that their large-distance properties would be the same for any potential with the same scattering length [31]. Without loss of generality we therefore choose a two-body square-well potential of depth, $V_0 > 0$, and radius, r_0, which for simplicity in the notation will be taken the same for each of the three pairwise interactions involved in the three-body system.

Different estimates can be made in order to fix the value of ρ_0 determining the upper limit of interval I. To do so, let us recall that the hyper-radius defined in Eq. (1) can also be written in terms of the usual $\boldsymbol{x}$ and $\boldsymbol{y}$ Jacobi coordinates, $\rho^2 = x^2 + y^2$, which is independent of the Jacobi set chosen to describe the system [7], and where $\boldsymbol{x} = \sqrt{\mu_{ij}/m}\,\boldsymbol{r}_{ij}$ and $\boldsymbol{y} = \sqrt{\mu_{ij,k}/m}\,\boldsymbol{r}_{ij,k}$ [μ_{ij} and $\mu_{ij,k}$ are the reduced masses of the ij and the $(ij)k$ systems, respectively, and $\boldsymbol{r}_{ij}$ and $\boldsymbol{r}_{ij,k}$ are their corresponding relative distances].

One possible estimate of ρ_0 can be made by taking it equal to the smallest of the three available values $\sqrt{\mu_{ij}/m}\,r_0$, which for three identical particles with mass m corresponds to $\rho_0 = r_0/\sqrt{2}$. This is the value of ρ obtained when $r_{ij,k} = 0$ and the distance between the other two is equal to r_0 (three aligned particles). This definition guarantees that for any geometry with $\rho < \rho_0$ the three pairs of particle-particle distances are smaller than r_0. However, with this choice we disregard geometries with $\rho > \rho_0$ but still with all the interparticle distances smaller than r_0. An alternative could be to proceed the other way around, that is, to construct ρ_0 assuming that two of the particles are at the same position, $r_{ij} = 0$, and take $r_{ij,k} = r_0$ (dimer-particle structure). This leads, for three identical particles of mass m, to $\rho_0 = \sqrt{2/3}\,r_0$, although in this case it is possible to find geometries with $\rho \leqslant \rho_0$ and some particle-particle distance larger than r_0 (for instance when $\rho = \rho_0 = \sqrt{2/3}\,r_0$ and $r_{ij,k} = 0$, we get that $r_{ij} = 2r_0/\sqrt{3}$). In any case, we can conclude that an appropriate choice for ρ_0 should be, for three identical particles with mass m, in the vicinity of $\rho_0 = r_0/\sqrt{2} \approx 0.7 r_0$ or $\sqrt{2/3}\,r_0 \approx 0.8 r_0$.

According to this, in the small-distance interval I, Eq. (2) reduces to the Schrödinger-like equation [7]

$$\left(-\frac{\partial^2}{\partial \rho^2} + \frac{\ell_d(\ell_d + 1)}{\rho^2} - k^2\right) f_{\mathrm{I}}(\rho) = 0, \qquad (4)$$

$$k = \sqrt{\frac{2m(V_{03} + E)}{\hbar^2}}, \qquad (5)$$

where f_{I} is the related wave function in this interval, and k is the wave number related to the present three-body problem. In Eq. (5), $V_{03} = 3V_0$, due to the presence of three particle-particle interactions within the three-body system.

The crucial intermediate interval, $\rho_0 < \rho < |a_{\mathrm{av}}|$, interval II, is upwards limited by $|a_{\mathrm{av}}|$, which for three arbitrary masses can be defined in analogy to Eq. (1),

$$mM a_{\mathrm{av}}^2 = \sum_{i<j} a_{ij}^2 m_i m_j, \qquad (6)$$

or perhaps as in Ref. [40]:

$$a_{\mathrm{av}} \sqrt{m} = \frac{\sqrt{2}}{3} \sum_{i<j} a_{ij} \sqrt{\mu_{ij}}, \qquad (7)$$

where μ_{ij} is the reduced mass of particle pairs i and j and a_{ij} is the d-dependent scattering length of the potential between particles i and j. Both definitions in Eqs. (6) and (7) have the merit of returning a_{av} as the initial two-body scattering length for three identical particles with mass m. Another definition may turn out to be more suitable for asymmetric systems, but the limit for identical particles must be maintained.

The necessary assumption here is that the supporting decoupled adiabatic potential is sufficiently accurate for our purpose. The Schrödinger equation is then

$$\left(-\frac{\partial^2}{\partial \rho^2} + \frac{\lambda_\infty + \ell_d(\ell_d + 1)}{\rho^2} - \frac{2m}{\hbar^2}E\right) f_{\mathrm{II}}(\rho)$$
$$= \left(-\frac{\partial^2}{\partial \rho^2} + \frac{-|\xi_d|^2 - 1/4}{\rho^2} - \kappa^2\right) f_{\mathrm{II}}(\rho) = 0, \qquad (8)$$

where f_{II} is the relative wave function in this interval, and the energy-related wave number, κ, is defined by

$$\kappa^2 = \frac{2mE}{\hbar^2}. \qquad (9)$$

The effective potential in Eq. (8) is given by the ρ-independent λ value at large distances, λ_∞, including the angular momentum term [7], and before the (large) scattering length is reached. The value of λ_∞ is determined by the universal nonanalytic imaginary solution, ξ_d, to a transcendental equation [7,12,41] depending on d and on the particular three-body system under investigation. The actual value of $|\xi_d|$ is closely related to the well-known scaling of energies and sizes of Efimov states [1,31]. The numerator in the centrifugal barrier term is then $\lambda_\infty + \ell_d(\ell_d + 1) \equiv \ell^*(\ell^* + 1)$, where $\ell^* = i|\xi_d| - 1/2$ is an effective complex angular momentum, again similar to the Regge pole analytic continuation [39].

This approximation of the adiabatic potential requires a large scattering length, $|a_{\mathrm{av}}|$, which is in complete agreement with the potential independence valid at distances far outside the short-range three-body potential. All assumptions are very well fulfilled for dimension d sufficiently close to d_E, where the two-body scattering length is infinitely large.

The potential in the third interval, interval III, at large distances outside the average scattering length, $\rho > |a_{\mathrm{av}}|$, is again taken from the general behavior of $\lambda(\rho)$ [7,12]. The Schrödinger equation is now in this interval:

$$\left(-\frac{\partial^2}{\partial \rho^2} + \frac{\ell_C(\ell_C + 1)}{\rho^2} - \kappa_C^2\right) f_{\mathrm{III}}(\rho) = 0, \qquad (10)$$

$$\kappa_C = \sqrt{\frac{2m}{\hbar^2}(E - C)}. \qquad (11)$$

The definitions of κ_C and ℓ_C are related to the characteristics of the three-body problem, and determined from the two possible behaviors of $\lambda(\rho)$ at large distance. The first possibility is $\lambda(\rho) \overset{\rho \to \infty}{\longrightarrow} 0$ ($C = 0$), which corresponds to the case when no two-body bound state exists, and for which we have $\kappa_C = \kappa$, Eq. (9), and $\ell_C = \ell_d = d - 3/2$. The change in the effective potential from interval II to interval III very likely implies that

the potential is discontinuous at $\rho = |a_{\mathrm{av}}|$, but still perfectly allowed in the equation of motion.

The second possibility is that $\lambda(\rho) \xrightarrow{\rho \to \infty} 2m\rho^2 E_2/\hbar^2$, and $C = E_2 < 0$, when an asymptotic two-body bound-state structure of binding energy, $|E_2|$, is approached. In this case $\kappa_C \neq \kappa$, and $\ell_C = (d-3)/2$, which is the d-dependent effective angular momentum quantum number associated to an ordinary two-body collision in d dimensions, namely, the collision between the third particle and the bound dimer.

It is important to keep in mind that in this analysis we are considering only one λ function, which amounts to considering only the first, usually dominant, term in the adiabatic expansion of the wave function [7]. This means in practice that we are restricting ourselves to scattering processes where the incoming and outgoing channels are described by the same λ function. In other words, if $\lambda \xrightarrow{\rho \to \infty} 0$ we are then dealing with a $3 \to 3$ process, where we have an unbound three-body system in the initial and final state. In contrast, if $\lambda \xrightarrow{\rho \to \infty} 2m\rho^2 E_2$, we are then dealing with an elastic-scattering process, where one of the particles hits the bound two-body state leading to the same particle + dimer system after the collision. We shall refer to these processes as $1 + 2 \to 1 + 2$ reactions. For both $3 \to 3$ and $1 + 2 \to 1 + 2$ processes, note that the dimensionless quantity $\kappa_C r_0$ is nothing but $\sqrt{E_{\mathrm{inc}}}$, where E_{inc} is the incident collision energy in units of $\hbar^2/(2mr_0^2)$, as one can immediately see from Eq. (11).

The description of other processes, like the recombination of three particles into a particle + dimer state, or breakup $1 + 2$ reactions, unavoidably requires the inclusion of additional open channels. This necessarily requires calculation of the full $\mathcal{S}$ matrix of the process [34,35]. This generalization will not be considered here.

B. Phase shifts

The wave functions are found by solving Eqs. (4), (8), and (10) in their respective intervals with subsequent matching at the boundaries, where both $\rho = 0$ and ∞ are included. The distance dependent inverse square effective potentials allow analytic solutions even though the strength sometimes is negative in contrast to the well-known centrifugal barrier solutions. We consider the case of continuum states, but the procedure can as well be applied to bound-state computations. The formal expressions for the radial solutions are

$$f_{\mathrm{I}}(\rho) \propto \rho j_{\ell_d}(k\rho), \tag{12}$$

$$f_{\mathrm{II}}(\rho) \propto \cot\delta_m \rho j_{\ell^*}(\kappa\rho) - \rho\eta_{\ell^*}(\kappa\rho), \tag{13}$$

$$f_{\mathrm{III}}(\rho) \propto \cot\delta_o \rho j_{\ell_C}(\kappa_C\rho) - \rho\eta_{\ell_C}(\kappa_C\rho), \tag{14}$$

where j_ℓ and η_ℓ are the spherical Bessel functions with the given indices and arguments. The indices may be continuous, like ℓ_d, or even complex, like ℓ^*, and the arguments may also take complex values. In any case, the analytic continuation of the Bessel functions guarantees unique definitions. The precise normalization is not relevant for our purpose. The continuous functions, δ_m and δ_o, are phase shifts as functions of energy for continuum solutions. We already inserted the

finite boundary condition at $\rho = 0$ for f_{I}, since $j_{\ell_d}(k\rho) \to 0$ for $\rho \to 0$, but $\eta_{\ell_d}(k\rho) \to \infty$ for $\rho \to 0$.

To find the relation to the still unknown constants, the phase shifts, we have to match the logarithmic derivatives at the two boundaries, ρ_0 and $|a_{\mathrm{av}}|$. The first one, the match at $\rho = \rho_0$, leads to

$$\frac{f_{\mathrm{I}}'(\rho_0)}{f_{\mathrm{I}}(\rho_0)} = \frac{f_{\mathrm{II}}'(\rho_0)}{f_{\mathrm{II}}(\rho_0)}, \tag{15}$$

where the prime means derivative with respect to ρ. After some algebra, and exploiting the well-known relations of the Bessel functions and their derivatives, one can easily obtain

$$\cot\delta_m = \frac{\kappa\rho_0\eta_{\ell^*+1}(\kappa\rho_0) + C_1\eta_{\ell^*}(\kappa\rho_0)}{\kappa\rho_0 j_{\ell^*+1}(\kappa\rho_0) + C_1 j_{\ell^*}(\kappa\rho_0)}, \tag{16}$$

where κ is from Eq. (9) and the constant, C_1, is given by

$$C_1 = (\ell_d - \ell^*) - k\rho_0 \frac{j_{\ell_d+1}(k\rho_0)}{j_{\ell_d}(k\rho_0)}. \tag{17}$$

In the same way, the second boundary matching at $\rho = |a_{\mathrm{av}}|$ imposes the condition

$$\frac{f_{\mathrm{II}}'(|a_{\mathrm{av}}|)}{f_{\mathrm{II}}(|a_{\mathrm{av}}|)} = \frac{f_{\mathrm{III}}'(|a_{\mathrm{av}}|)}{f_{\mathrm{III}}(|a_{\mathrm{av}}|)}, \tag{18}$$

which, similarly to Eq. (16), leads to

$$\cot\delta_o = \frac{\kappa_C|a_{\mathrm{av}}|\eta_{\ell_C+1}(\kappa_C|a_{\mathrm{av}}|) + C_2\eta_{\ell_C}(\kappa_C|a_{\mathrm{av}}|)}{\kappa_C|a_{\mathrm{av}}|j_{\ell_C+1}(\kappa_C|a_{\mathrm{av}}|) + C_2 j_{\ell_C}(\kappa_C|a_{\mathrm{av}}|)}, \tag{19}$$

where the constant C_2 is given by

$$
\begin{aligned}
C_2 = {} & (\ell^* - \ell_C) \\
& - \kappa|a_{\mathrm{av}}| \frac{\cot\delta_m j_{\ell^*+1}(\kappa|a_{\mathrm{av}}|) - \eta_{\ell^*+1}(\kappa|a_{\mathrm{av}}|)}{\cot\delta_m j_{\ell^*}(\kappa|a_{\mathrm{av}}|) - \eta_{\ell^*}(\kappa|a_{\mathrm{av}}|)}.
\end{aligned}
\tag{20}
$$

It is important to keep in mind that the precise values of κ_C and ℓ_C in Eq. (19), coming from the outer interval in Eq. (10), depend on the existence or not of a bound two-body dimer. When the dimer is present, we then have $\kappa_C = \kappa_{C=E_2} \neq \kappa$ and $\ell_C = (d-3)/2 \neq \ell_d$, whereas, if it is not, then $\kappa_C = \kappa_{C=0} = \kappa$ and $\ell_C = \ell_d = d - 3/2$.

C. Low-energy expansion

Let us first consider the case when there is no bound dimer, and therefore $\kappa = \kappa_C$. In this case the low-energy assumption amounts to $\kappa \to 0$ and $\kappa_C \to 0$.

By expanding the Bessel functions around small arguments, the leading term in the expansion for $\cot\delta_m$, Eq. (16), leads to

$$\cot\delta_m \approx -\frac{[(2\ell^*+1)!!]^2}{(\kappa\rho_0)^{2\ell^*+1}} \left(\frac{1}{C_1} + \frac{1}{2\ell^*+1} \right). \tag{21}$$

In the expression for C_1, Eq. (17), we should insert $k \approx \sqrt{2mV_{03}/\hbar^2}$, as obtained from Eq. (5) when $E \to 0$. The expression in Eq. (21) can be generalized for noninteger ℓ^* as

$$\cot\delta_m \approx -\frac{[2^{\ell^*}\Gamma(\ell^*+1/2)(2\ell^*+1)]^2}{\pi(\kappa\rho_0)^{2\ell^*+1}} \left(\frac{1}{C_1} + \frac{1}{2\ell^*+1} \right). \tag{22}$$

In the same way, since $\kappa_C \to 0$, we can also perform the low-energy expansion of $\cot \delta_o$ in Eq. (19), which leads to expressions analogous to the ones in Eqs. (21) and (22), that is,

$$\cot \delta_o \approx -\frac{[(2\ell_C + 1)!!]^2}{(\kappa_C |a_{\mathrm{av}}|)^{2\ell_C + 1}} \left(\frac{1}{C_2} + \frac{1}{2\ell_C + 1} \right), \quad (23)$$

which for noninteger ℓ_C takes the form

$$\cot \delta_o \approx -\frac{[2^{\ell_C} \Gamma(\ell_C + 1/2)(2\ell_C + 1)]^2}{\pi (\kappa_C |a_{\mathrm{av}}|)^{2\ell_C + 1}} \left(\frac{1}{C_2} + \frac{1}{2\ell_C + 1} \right). \quad (24)$$

Expanding again the Bessel functions in Eq. (20) we get for C_2 that

$$C_2 = (\ell^* - \ell_C)$$
$$- \frac{[(2\ell^* + 1)!!]^2(2\ell^* + 1)}{[(2\ell^* + 1)!!]^2 + \cot \delta_m (2\ell^* + 1)(\kappa |a_{\mathrm{av}}|)^{(2\ell^* + 1)}}, \quad (25)$$

where the expansion for $\cot \delta_m$ from Eq. (21) can be inserted to give

$$C_2 = (\ell^* - \ell_C)$$
$$- \frac{(2\ell^* + 1)}{1 - (1 + (2\ell^* + 1)/C_1)(|a_{\mathrm{av}}|/\rho_0)^{2\ell^* + 1}}, \quad (26)$$

which is independent of κ, and therefore on the energy as well.

In the second scenario a bound dimer exists, and the low-energy limit then refers to a small particle-dimer collision energy, i.e., $E - E_2 \to 0$. From Eq. (11) it then immediately follows that $\kappa_{C=E_2} \to 0$, which implies that Eq. (24) is still valid in this case. Since κ is given by Eq. (9), we then have that in this low-energy limit $\kappa \approx \sqrt{-2m|E_2|/\hbar^2}$, which is a purely imaginary number.

In the case of three identical particles with mass m, and a sufficiently small value of $|E_2|$, we know that $|E_2| \approx \hbar^2/(ma_{\mathrm{av}}^2)$, which in the low-energy limit, leads to $\kappa |a_{\mathrm{av}}| \approx i\sqrt{2}$. Therefore, in this case Eq. (20) becomes

$$C_2 = (\ell^* - \ell_C) - i\sqrt{2} \frac{\cot \delta_m j_{\ell^* + 1}(i\sqrt{2}) - \eta_{\ell^* + 1}(i\sqrt{2})}{\cot \delta_m j_{\ell^*}(i\sqrt{2}) - \eta_{\ell^*}(i\sqrt{2})}. \quad (27)$$

In summary, at both thresholds we obtain $\cot \delta_o$ after insertion into Eq. (24) of the appropriate of the two C_2 expressions, either Eq. (26) or Eq. (27).

The low-energy limit in Eq. (24), or more precisely, the low-energy limit of $\kappa_C^{2\ell_C + 1} \cot \delta_o$, is related to the three-body scattering length, a_{3b}:

$$\lim_{\kappa_C \to 0} \kappa_C^{2\ell_C + 1} \cot \delta_o = -\frac{1}{a_{3b}^{2\ell_C + 1}}, \quad (28)$$

which characterizes the zero-energy scattering, and in two-body physics is also the measure of the cross section. It is formally related to the zero-energy limit of the phase shift. The small energy expansion (24), implying small phase shift, concludes that $(\kappa_C |a_{\mathrm{av}}|)^{2\ell_C + 1} \cot \delta_o \equiv -1/A_{3b}$, where

A_{3b} is a constant independent of energy, but a function of the dimension, d, the square-well parameter, $m\rho_0^2 V_{03}/\hbar^2$, and the average two-body scattering length, a_{av}/ρ_0, in units of ρ_0. From Eq. (28) it is then simple to see that $a_{3b}/|a_{\mathrm{av}}| = A_{3b}^{1/(2\ell_C + 1)}$.

The limiting phase shift is traditionally given as a power of the scattering length multiplied by the wave number. Since $\cot \delta_o$ diverges as $1/\delta_o$ in the zero-energy limit, we can explicitly define $\delta_o \to -A_{3b}(\kappa_C |a_{\mathrm{av}}|)^{2\ell_C + 1} = -(\kappa_C a_{3b})^{2\ell_C + 1}$. The resulting phase shift, δ_o, is in both cases (existence of bound dimer or not) approaching zero as a power of energy. The power is determined by $2\ell_C + 1 = 2d - 2$ when no dimer exists ($\kappa = \kappa_C \to 0$), and $2\ell_C + 1 = d - 2$ when a bound two-body state is present ($\kappa_C \to 0$ and κ is finite and imaginary).

D. Universality

In Ref. [17] two-body systems were discussed analytically for noninteger dimensions and general short-range potentials. The method was to refer numerical calculations to use of a square-well potential, where its radius, r_0, and depth, V_0, are found by the conditions that the ratio between the scattering length and effective range in three dimensions is identical to the same ratio for the given short-range potential. In this sense, the results provided in Ref. [17] for two-body systems were found to have universal character. The appearance of the two-body effective range as the length unit to be used to get universality is consistent with additional findings at the three-body level, where the two-body effective range is also found to be the relevant length scale unit setting a universal value for the three-body parameter [45]. Furthermore, for a given potential shape, any potential with the same value of $r_0^2 V_0$ does actually preserve the ratio between the scattering length and effective range.

At this point we can also wonder about the universal character of the expressions derived above for three-body systems. We can perhaps expect that such a universal character, understood as giving rise to equal results for different two-body interactions, is also related to the fact of producing the same ratio between the three-body scattering length and effective range for $d = 3$, as found for two-body systems. However, this way of determining the equivalence between different potentials is at least not very efficient, since it requires one to solve for all of them the numerical three-body problem for $d = 3$ and for very small energies, which could in itself be quite delicate.

The present investigation of the effects of an external deformed field turns actually the focus on noninteger dimensions close to the one, d_E, for which the Efimov effect occurs. For this reason, even more crucial than producing the same ratio between the scattering length and effective range at the three-body level, is that the potentials, in order to be considered equivalent, should provide the same Borromean d region for the three-body system, or at least the same value of the critical dimension, d_E, where the Efimov effect can appear. This last demand, having the same d_E value, has the advantage that it can be checked at the two-body level, since d_E is determined by the dimension at which a bound two-body state with zero energy is present. For this reason, in this paper we shall

consider that two short-range potentials are equivalent when providing the same critical dimension, d_E.

This choice for the definition of equivalent two-body potentials is in some way the natural choice. Formally, the division of the ρ space into three intervals, the extraction of the Schrödinger equation applying to each of them, and all the subsequent derivations have been performed assuming square-well two-body potentials. This affects interval I, where the effective three-body potential, Eq. (4), is also a square well the depth of which, dictated by the depth of the two-body potentials, enters explicitly in the definition of the wave number in Eq. (5). However, the shape of the potential is not relevant here, since the depth, through k in Eq. (4), only modifies the inner part of the wave function. What is really crucial is the size of the second interval, which is determined by the value of the average two-body scattering lengths, $|a_{av}|$. This is the region where the effective three-body potential is essentially given by the asymptotic value of the λ function, i.e., λ_∞, which is potential independent, and which determines the scaling of the Efimov states. Therefore, no matter the shape of the two-body potentials, two different potentials having the same large scattering length for a given dimension will provide the same series of scaled Efimov states, and, therefore, they will give rise to very similar three-body wave functions. For this same reason, if two different two-body potentials produce the same critical dimension d_E (infinite two-body scattering length), it is then obvious that for any dimension close to d_E both potentials will have pretty similar large scattering lengths, and again the corresponding three-body wave functions will be similar as well.

The conclusion is then that, provided that we are dealing with dimensions close to d_E, the analytic expressions derived in the previous subsections can be applied to any short-range two-body potential with critical dimension d_E, not just a square-well potential. The only thing one has to do is to provide the correct $|a_{av}|$ value for each dimension, and, for the case of $1 + 2 \rightarrow 1 + 2$ reactions, also the correct binding for the bound dimer. The value of the depth, V_0, and therefore the value of V_{03} in Eq. (4), can be estimated as an average of the depth in the inner part of the potential, or just the value of the two-body potential at the origin.

In any case, no matter the shape of the two-body potentials, in order to be able to find analytic solutions, we aim in interval I at an effective three-body square-well potential in terms of the hyper-radius, with depth, V_{03}, and a range, ρ_0. In particular, for three identical particles we have that $V_{03} = 3V_0$. The three-body square-well radius, ρ_0, should reflect the two-body short-range properties, although at most this is possible to achieve on average. In this paper two different estimates of ρ_0 have been proposed, which consist of different average radii for the geometry of three particles in different arrangements such that the three interparticle distances are smaller than the range of the two-body potentials.

Once the value of V_{03} and ρ_0 to be used in the analytic equations is determined, the three-body properties might as well be obtained by any ρ_0, even very small and approaching zero range, provided the corresponding hyper-radial depth is accordingly adjusted. The relation can be taken analogous to the two-body result, which leads to an approximately constant value of the combination $\rho_0^2 V_{03}$. All these possibilities can be

tested and corresponding dimensions can be calculated for any set of short-range two-body interactions. These choices of parameters extend the applications for specific interactions to universal properties.

III. RESULTS

Although the analytic derivations in the section above are general, it is obvious that numerical applications demand choosing specific systems. For the present first exploratory investigation we select the example of three identical spinless particles. The mass of the particles is taken equal to the normalization mass, m. This choice has the advantage of being the system with fewest degrees of freedom, since all three two-body interactions and mass ratios are identical. In any case, asymmetric systems can also be studied numerically with the general formalism developed in the previous section.

For the particle-particle interaction we choose the Gaussian potential described in Ref. [16] for the case of identical particles. As shown in Ref. [16], after full numerical calculations, this interaction is such that the three-body system is not bound for $d = 3$, but after some squeezing, for $d \approx 2.89$, the first bound three-body state shows up. The critical dimension d_E for this potential is $d_E = 2.75$, where a two-body bound state appears with zero energy. This implies that for dimensions within the range $2.75 \leqslant d \lesssim 2.89$ the three-body system has Borromean character, whereas for $d < d_E = 2.75$ bound two-body dimers are always present. For $d \approx 2.76$ the first bound three-body excited state appears. The results to be shown later on with this potential will be compared with the ones obtained with the equivalent two-body square-well potential providing the same critical dimension, $d_E = 2.75$, as in the Gaussian case.

A. Three-body potential

Let us start by investigating the characteristics of the effective three-body ρ-dependent potential entering in Eq. (2), which is given by Eq. (3). The procedure followed in order to construct this potential in the schematic model contains two important approximations. First, only one of the adiabatic hyperspherical potentials is used, where all the coupling terms are assumed small and neglected. And second, the coordinate space is divided into three well-defined ρ intervals, each of them containing a very specific d-dependent centrifugal barrier.

The small-ρ region, interval I, is of little importance and could as well be disappearingly narrow to the limit of a zero-range potential with correspondingly adjusted attractive strength. In this region, the effective potential in Eq. (3) becomes

$$U_{\text{eff}} = \frac{\ell_d(\ell_d + 1)}{\rho^2} - \frac{2mV_{03}}{\hbar^2}, \tag{29}$$

as extracted from Eq. (4).

The intermediate region, interval II, is chosen to be that of the asymptotic large-distance behavior of the $\lambda(\rho)$ function close to occurrence of the Efimov effect, that is, the $\rho_0 \ll \rho \ll |a_{av}|$ region where $\lambda(\rho) = \lambda_\infty$ takes a constant value. Here, as
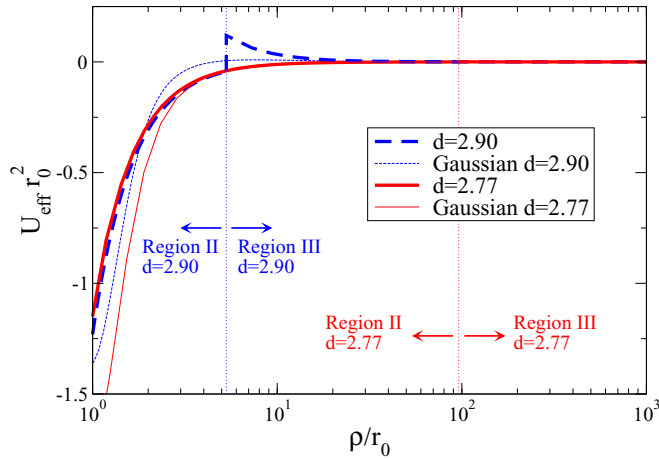
FIG. 1. Three-body effective potential in intervals II and III for three identical bosons for $d = 2.90$ (dashed curves) and $d = 2.77$ (solid curves). The division between intervals II and III is shown by the vertical dotted lines for each of the d values. The range to the two-body interaction, r_0, is taken as length unit. The mass of the particles is equal to the normalization mass. The thin curves are full three-body calculations using the Gaussian potential as described in Ref. [16]. The thick curves are the result from Eqs. (30) and (31) using the $|a_{av}|$ values of the same Gaussian potential.

seen in Eq. (8), the effective potential takes the form

$$U_{\text{eff}} = \frac{-|\xi_d|^2 - \frac{1}{4}}{\rho^2}. \tag{30}$$

Finally, in the large distance region, interval III, the effective potential is given by the ordinary centrifugal barrier, but shifted by zero energy or by the energy corresponding to the possible two-body bound state, as determined by the value of C in Eq. (11). This is shown in Eq. (10), from which we get that in this interval we have

$$U_{\text{eff}} = \frac{\ell_C(\ell_C + 1)}{\rho^2} + \frac{2mC}{\hbar^2}. \tag{31}$$

In order to compare the schematic effective potential described by Eqs. (29), (30), and (31), and the one obtained in a realistic three-body calculation [16], we use the Gaussian potential introduced at the beginning of this section. We choose two different dimensions, $d = 2.90$ and 2.77, which are, respectively, rather far from or close to the critical dimension $d_E = 2.75$. For the Gaussian potential used, we have that $|a_{av}| = 5.3$ and 96.2 (both in units of the range of the two-body interaction, r_0) for $d = 2.90$ and 2.77, respectively. This implies that the second interval in our model, $\rho_0 < \rho < |a_{av}|$, is pretty small for $d = 2.90$, whereas for $d = 2.77$ it is sufficiently large to expect that the $\lambda(\rho)$ function in Eq. (2) reaches the asymptotic value $\lambda_\infty = -|\xi_d|^2 - (d-1)^2$ within the region [see Eq. (8)]. In particular, we have that $|\xi_d|^2$ is equal to 0.978 and 0.879 for $d = 2.90$ and 2.77, respectively.

In Fig. 1 the thin-dashed (blue) and thin-solid (red) curves show the lowest effective potential in Eq. (3), times r_0^2 to make

it dimensionless, obtained after a full three-body calculation, as described in Ref. [16], for $d = 2.90$ and 2.77, respectively. The vertical dotted lines indicate the value of $|a_{av}|$ for each of the two cases. These lines determine the separation between intervals II and III in the schematic model. As seen in Eqs. (30) and (31), in these two intervals the effective potential provided by the schematic model is dictated just by $|\xi_d|$ and d (for the dimensions chosen we have that $\ell_C = \ell_d = d - 3/2$ and $C = 0$), reflecting the fact that in these two regions, II and III, the details of the two-body interaction are unimportant. Only in region I, as seen in Eq. (29), the strength of the potential enters. However, as already mentioned, the behavior of the effective potential in this region has little relevance, since our conclusions entirely are based on large-distance properties of the potentials. For this reason only intervals II and III are shown in the figure.

In the figure the thick-dashed (blue) and thick-solid (red) curves show the result for the effective potential arising from Eqs. (30) and (31) for $d = 2.90$ and 2.77, respectively. We can immediately see that, for $d = 2.90$ (dashed curves), the schematic model provides a potential that differs clearly from the one obtained after a full calculation. In fact the transition between regions II and III is quite abrupt. This is related to the fact that for this dimension the scattering length is too small (we are far from the Efimov conditions), meaning that region II is too small as well, and the conditions for the validity of Eq. (30) in such region are not properly fulfilled.

In fact, for $d = 2.77$, for which the value of $|a_{av}|$ is significantly larger than the range of the interaction, r_0, we can see that the computed potential, thin-solid red, and the one provided by Eq. (30), thick-solid red, become soon indistinguishable, and the abrupt transition from interval II to interval III cannot be seen.

We can therefore conclude that the analytic model effective potential and the realistic potential are almost identical for dimensions close to d_E and for hyper-radii larger than two to three times the interaction radius. For a given dimension, d, the potential is essentially determined by the value of ξ_d.

B. Phase shifts

The value of $\cot \delta_o$, which is a function of d, is a key quantity that reflects the presence of three-body bound states and resonances, as well as for the cross sections. More precisely, the zeros of $(\kappa_C a_{av})^{2\ell_c+1} \cot \delta_o$ in the $E \to 0$ limit indicate the appearance of zero-energy bound three-body states, since these zeros correspond to infinite three-body scattering length.

To investigate the validity of the results given in Eq. (19) or (23), which are indistinguishable in the low-energy limit, we show in Fig. 2, as a function of d, the value of $(\kappa_C |a_{av}|)^{2l+1} \cot \delta_o$ as obtained from those equations for $E \approx 0$ and after introducing the strength, V_{03}, and a_{av} values corresponding to the two-body potentials. As mentioned, we consider the Gaussian two-body potential given in Ref. [16] (thick curves) and the equivalent (same d_E value) square-well potential (thin curves). In Eqs. (19) and (23), the only parameter not fully determined by the dimension, d, and the interaction used, is the upper limit of interval I, i.e., the value of ρ_0. Two different possibilities were suggested in Sec. II,
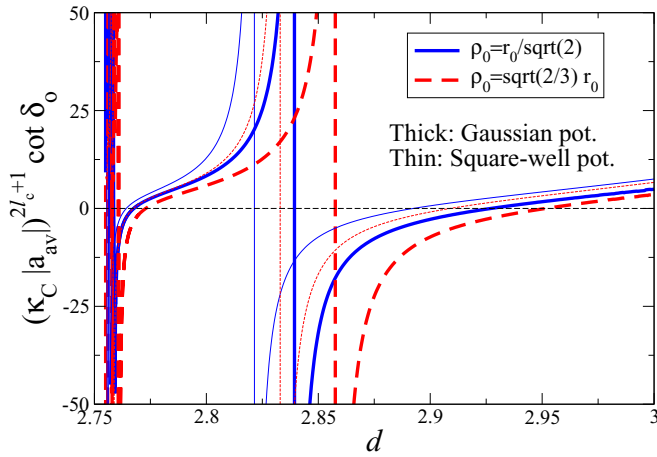
FIG. 2. For the Gaussian potential in Ref. [16] (thick curves) and the equivalent (same d_E value) square-well potential (thin curves), the three-body value of $(\kappa_C |a_{\mathrm{av}}|)^{2\ell_c+1} \cot \delta_o$, as a function of d, for $d > d_E = 2.75$ and $E \rightarrow 0$, as obtained from Eq. (19). The solid and dashed curves are the results obtained with $\rho_0 = r_0/\sqrt{2}$ and $\sqrt{2/3}r_0$, respectively.

$\rho_0 = r_0/\sqrt{2}$ and $\sqrt{2/3}r_0$, which correspond to the solid and dashed curves in Fig. 2, respectively.

We restrict ourselves in the figure to the region $d > d_E$, since this is the region where, when starting the confinement from $d = 3$ towards smaller values of d, the different bound three-body states progressively appear. In the figure we can see that when moving down from $d = 3$, we find the first zero at $d \approx 2.93$ or 2.95, depending on the value of ρ_0 used, for the Gaussian potential, and at $d \approx 2.89$ or 2.91, for the same ρ_0 values, with the square-well potential. This one should then be the dimension for which the first three-body bound state is found. As already mentioned, after a full three-body calculation with the Gaussian potential, as shown in Ref. [16], we have found that the first bound state does actually appear at $d \approx 2.89$. This value agrees reasonably well with the zero of all the functions in Fig. 2, although, especially for the Gaussian case, some discrepancy is observed. This discrepancy is however not dramatic, since for $d \approx 2.90$, as seen in Fig. 1, the schematic effective potential and the one obtained in the full calculation clearly differ in region II, and the schematic model is expected not to work very well. In fact, if we keep moving down to smaller values of d, we observe a second zero, and therefore the first three-body excited bound state, at a dimension that, in all the cases, ranges between $d \approx 2.76$ and 2.77. This is as well the value quoted in Ref. [16] as the one for which the first excited state is found after the full three-body calculation.

When still moving down to dimensions close to $d = d_E$, more and more, and eventually infinitely many, bound states appear. This leads to very rapid oscillations of $(\kappa_C |a_{\mathrm{av}}|)^{2\ell_c+1} \cot \delta_o$ and to an accumulation of zeros around $d = d_E$ which are very difficult to obtain numerically.

The result shown in Fig. 2 is very reassuring, making us confident on the validity of the low-energy limit of Eq. (19), as well as on the equivalence between the Gaussian potential and the square well with the same d_E value in the same low-energy

limit. To investigate its validity for a larger energy range, we focus now on the phase shifts as a function of the energy [or κ_C, Eq. (11)] for fixed values of the dimension. This is shown in Fig. 3, where the different panels show the phase shift δ_o as a function of $\kappa_C r_0$ for several values of d close to $d_E = 2.75$, which is the region where Eq. (19) is expected to work.

The phase shifts are of course undetermined by a phase of $180°$, and typically they are given to range either between -90 and $90°$, or between 0 and $180°$. However, to avoid sudden jumps in the curves, we have in Fig. 3 allowed the phase shifts to reach values beyond $180°$ or smaller than $-90°$. In this way, when decreasing the energy, all the curves will show a smooth increase towards $180°$ (which is equivalent to $0°$), being occasionally bigger than this value. The only exception will be panel (f), where the phase shifts are always within the 0 to $180°$ range.

The upper panels (a), (b), and (c) correspond to cases where $d < d_E$, describing then $1 + 2 \rightarrow 1 + 2$ reactions. In these panels the vertical dotted line indicates the $\kappa_C r_0$ value corresponding to the two-body breakup threshold when the Gaussian potential is used (when the equivalent square-well potential is used the corresponding vertical lines can hardly be distinguished from the ones shown in the figure). The lower panels (d), (e), and (f), for which $d > d_E$, describe $3 \rightarrow 3$ reactions.

In the figure the thick and thin curves are, respectively, the results obtained using the Gaussian and the equivalent square-well potentials, whereas, for each of them, the solid and dashed curves show the results obtained from Eq. (19) with $\rho_0 = r_0/\sqrt{2}$ and $\sqrt{3/2}r_0$, respectively. The brown dots are the results obtained from a full numerical three-body calculation with the Gaussian potential, where the radial wave function associated to the lowest adiabatic potential is calculated for the different $\kappa_C r_0$ values up to a distance of $\rho_{\max} \approx 500 r_0$. After fitting this wave function with the asymptotic behavior given in Eq. (14) the value of δ_o is then extracted. For $\kappa_C r_0$ values in the vicinity of or smaller than about 0.1 the correct asymptotic behavior of the numerical wave function is reached beyond the chosen value of $\rho_{\max} \approx 500 r_0$, and the extraction of the phase shift would require a more accurate three-body calculation. In any case, especially for $1 + 2 \rightarrow 1 + 2$ reactions below the two-body breakup threshold this numerical procedure is very inefficient and very likely even numerically impossible, being then necessary to implement an alternative [36,37].

As we can see in the figure, for both $1 + 2 \rightarrow 1 + 2$ (upper panels) and $3 \rightarrow 3$ (lower panels) reactions, the agreement between the numerical phase shifts (brown dots), in the energy region where they can be easily computed, and the analytic calculations from Eq. (19) is remarkably good. This is especially true when choosing $\rho_0 = \sqrt{2/3}r_0$ (dashed curves), which then appears as a better choice for the upper limit of interval I. The other choice, $\rho_0 = r_0/\sqrt{2}$ (solid curves), is perhaps too restrictive, eliminating from interval I a bit too much of the three-body geometries containing the three particles within the potential range. This result is therefore consistent with the spatial structure of Efimov states, that is a coherent superposition of the three dimer-particle configurations, as also found in detailed analyses investigating their spatial structure [42–44].
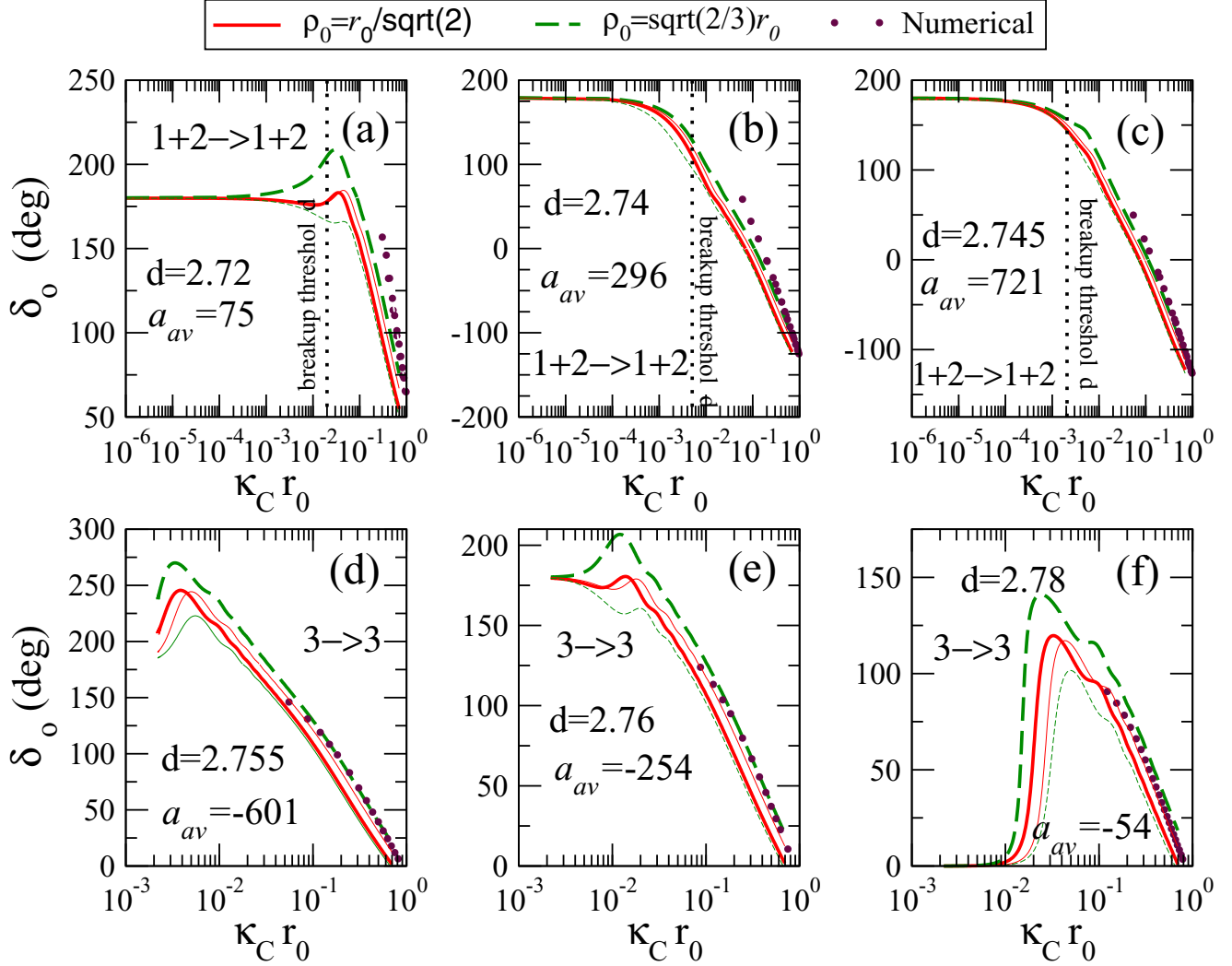
FIG. 3. For the Gaussian potential used in this paper (thick curves) and the equivalent (same d_E value) square-well potential (thin curves), three-body phase shift, δ_o, in degrees, as a function of $\kappa_C r_0$ for different values of d in the vicinity of d_E. The solid and dashed curves are the results obtained from Eq. (19) with $\rho_0 = r_0/\sqrt{2}$ and $\sqrt{3/2}r_0$, respectively. The (brown) dots are the results obtained from full numerical three-body calculations with the Gaussian potential. The cases in the upper and lower rows correspond to $1 + 2 \rightarrow 1 + 2$ ($d < d_E = 2.75$) and $3 \rightarrow 3$ ($d > d_E = 2.75$) reactions, respectively. In the upper panels the vertical dotted line indicates the two-body breakup threshold (very similar with both potentials). The scattering length a_{av} quoted in the figure for each of the cases, obtained with the Gaussian potential, is in units of r_0.

Also, the results obtained from the Gaussian potential (thick curves) and the equivalent square-well potential (thin curves) are very similar, often indistinguishable from each other. This fact supports the universal validity of Eq. (19) after defining the equivalent potentials as those giving rise to the same critical dimension, d_E. This definition actually makes particular sense if we recall that Eq. (19) has been designed to work for dimensions in the vicinity of d_E. In fact, the largest discrepancies between the different curves in Fig. 3 are observed in panels (a) and (f), which are as well the cases for which the dimension, $d = 2.72$ and 2.78, differs the most from $d_E = 2.75$.

The conclusion is then that the semianalytic procedure described in this paper provides reliable results for the phase shifts in the region close to $d = d_E$, where the Efimov conditions are close to being fulfilled. This is like this for both $1 + 2 \rightarrow 1 + 2$ and $3 \rightarrow 3$ reactions, and the phase shifts can

be obtained even for extremely small energies. This is particularly relevant for elastic $1 + 2 \rightarrow 1 + 2$ collisions below the two-body breakup threshold, since, due to the small dimer energies for $d \lesssim d_E$, the allowed collision energies, or the $\kappa_C r_0$ values, are extremely small as well, which makes the full numerical calculation very delicate.

IV. APPLICATION IN THREE DIMENSIONS

The d method has been presented as an efficient procedure to describe a system subject to the presence of a confining external potential. The great advantage is that the deformed external field is replaced by a dimension dependent angular momentum barrier in spherical calculations. However, in order to compare with the available experimental data, for instance with measured cross sections, it is necessary to translate the d-dimensional wave functions into the or-

dinary three-dimensional, squeezed, space. This is done by directly interpreting the d-wave function as a wave function in three dimensions, but deformed along the squeezing direction [13–15].

A. Scaling and external field

The starting point in all the derivations in Sec. II is Eq. (2), which amounts to assuming that only one, decoupled, adiabatic channel is enough to describe the system. For large values of the hyper-radius, ρ, this equation becomes Eq. (10), which formally describes a one-body problem with angular momentum, ℓ_C, where initial and final states correspond to infinitely large ρ. The underlying structure of three particles does not enter in the calculations, but only through the subsequent interpretation, where the relative coordinate, ρ, is the connection.

As mentioned, the inclusion of just one channel implies that only elastic processes can be described within the model, that is, the incoming and outgoing channel are the same. In other words, only two processes are possible. The first one corresponds to elastic scattering of one of the particles on the other two in a bound state, that is, $1 + 2 \rightarrow 1 + 2$ reactions. The second one is the theoretical construction of simultaneous elastic scattering of three particles in a continuum state described by one decoupled adiabatic hyperspherical potential, that is, $3 \rightarrow 3$ reactions. These cases correspond to the large-distance Schrödinger equation in Eq. (10), where κ_C is from Eq. (11), and (ℓ_C, C) is given by $(\ell_C = (d - 3)/2, C = E_2)$ or $(\ell_C = \ell_d = d - 3/2, C = 0)$ for the first and the second case, respectively. The interactions are contained in the Schrödinger equations for the intermediate- and short-distance intervals.

Following what is done in Ref. [17] for two-body systems, and taking the z axis along the squeezing direction, we interpret the hyper-radius ρ in the d space, as the hyper-radius in the three-dimensional space, $\tilde{\rho}$, but deformed along the z axis by means of a scale parameter, s (see Ref. [15] for details):

$$\rho \rightarrow \tilde{\rho} = \sqrt{\rho_x^2 + \rho_y^2 + \frac{\rho_z^2}{s^2}} = \sqrt{\rho_\perp^2 + \frac{\rho_z^2}{s^2}}. \quad (32)$$

The connection between the dimension, d, and the scale parameter, s, was in Ref. [15] estimated to be given by

$$\frac{1}{s^2} = \left[1 + \left(\frac{(3 - d)(d - 1)}{2(d - 2)} \right)^2 \right]^{1/2}, \quad (33)$$

which is based on the assumption of harmonic oscillator particle-particle interaction [15].

In this way the computed d-dimensional wave function, $\Psi_d(\rho)$, can be understood as a wave function in the three-dimensional space, $\tilde{\Psi}(\rho_\perp, \rho_z, s)$. As done in Ref. [15], $\tilde{\Psi}$ can then be expanded in terms of some convenient three-dimensional orthonormalized basis set, which, in general, could depend on the hyper-radius, $\rho = \sqrt{\rho_\perp^2 + \rho_z^2}$, and the usual five hyperangles, Ω:

$$\tilde{\Psi}(\rho_\perp, \rho_z, s) = \frac{1}{\rho^{5/2}} \sum_n \tilde{f}_n(\rho, s) \Phi_n(\rho, \Omega). \quad (34)$$

From the expression above it is simple to extract the radial wave functions in the three-dimensional (squeezed) space,

which are given by

$$\tilde{f}_n(\rho, s) = \rho^{5/2} \int d\Omega \tilde{\Psi}(\rho_\perp, \rho_z, s) \Phi_n^*(\rho, \Omega), \quad (35)$$

where $d\Omega$ is the usual phase space associated with the hyperangles for three particles in three dimensions and n numbers the different terms of the basis set, $\{\Phi_n\}$. This same procedure was used in Ref. [15] for the case of bound states.

Calculation of the radial wave functions (35) is particularly simple when, as done in this paper, only s waves enter in the d-dimensional wave function, and only the lowest adiabatic channel is considered. If, furthermore, we choose the basis set, $\{\Phi_n\}$, as the one formed by the usual hyperspherical harmonics, the two integrals in Eq. (35) involving the azimuthal angles of the Jacobi coordinates can be done analytically, and only the three remaining hyperspherical angles have to be integrated away numerically. Even more, for large values of ρ, the radial part contained in $\tilde{\Psi}$ can be replaced by the known asymptotic form in Eq. (14), although, as discussed in Ref. [17], in order to guarantee the confinement along the z axis, it has to be multiplied by a factor $e^{-\rho_z^2/(2b_{HO}^2)}$. Here, b_{HO} is the harmonic oscillator length associated to the squeezing potential, which can be related to the dimension d as given in Refs. [15,17].

Also, each term n of the hyperspherical basis set has associated a value K of the hypermomentum, in such a way that the asymptotic behavior of the radial wave functions in Eq. (35) should, in principle, take the form

$$\tilde{f}_n(\rho, s) \xrightarrow{\rho \rightarrow \infty} \cot \delta_n \rho j_{K + \frac{3}{2}}(\kappa_C \rho) - \rho \eta_{K + \frac{3}{2}}(\kappa_C \rho), \quad (36)$$

from which the three-dimensional phase shift δ_n can be extracted.

As discussed in Ref. [17], the asymptotic behavior in Eq. (36) corresponds to the usual, nondeformed, three-dimensional space. Therefore the phase shift, δ_n, obtained from it, should not necessarily be the one in the squeezed space. In fact, without any interaction between the particles, the phase shift obtained in the d formalism is trivially equal to zero ($\delta_o = 0$) and the corresponding d-dimensional radial wave function is just $\rho j_{\ell_C}(\kappa_C \rho)$, which means $\tilde{\Psi} \propto \tilde{\rho} j_{\ell_C}(\kappa_C \tilde{\rho})$. Comparison of the radial wave functions then obtained through Eq. (35) and the asymptotic behavior (36) gives rise to a nonzero phase shift, δ_{free}. Therefore, the correct phase shift in the confined space, δ_{conf}, should be the difference between the computed phase shift, δ_n, and the one corresponding to the free case, δ_{free}. In other words, we have that

$$\delta_{\text{conf}} = \delta_n - \delta_{\text{free}}. \quad (37)$$

B. The $1 + 2 \rightarrow 1 + 2$ reactions

In Ref. [17] we have shown that, for two-body reactions, the phase shifts obtained with the d method are the same as the phase shift, δ_{conf}, obtained as described above. The consequence is that the phase shifts obtained with the d method can be directly used in the usual expressions for elastic cross sections. This is particularly relevant for $1 + 2 \rightarrow 1 + 2$ reactions, since they are formally identical to a two-body problem
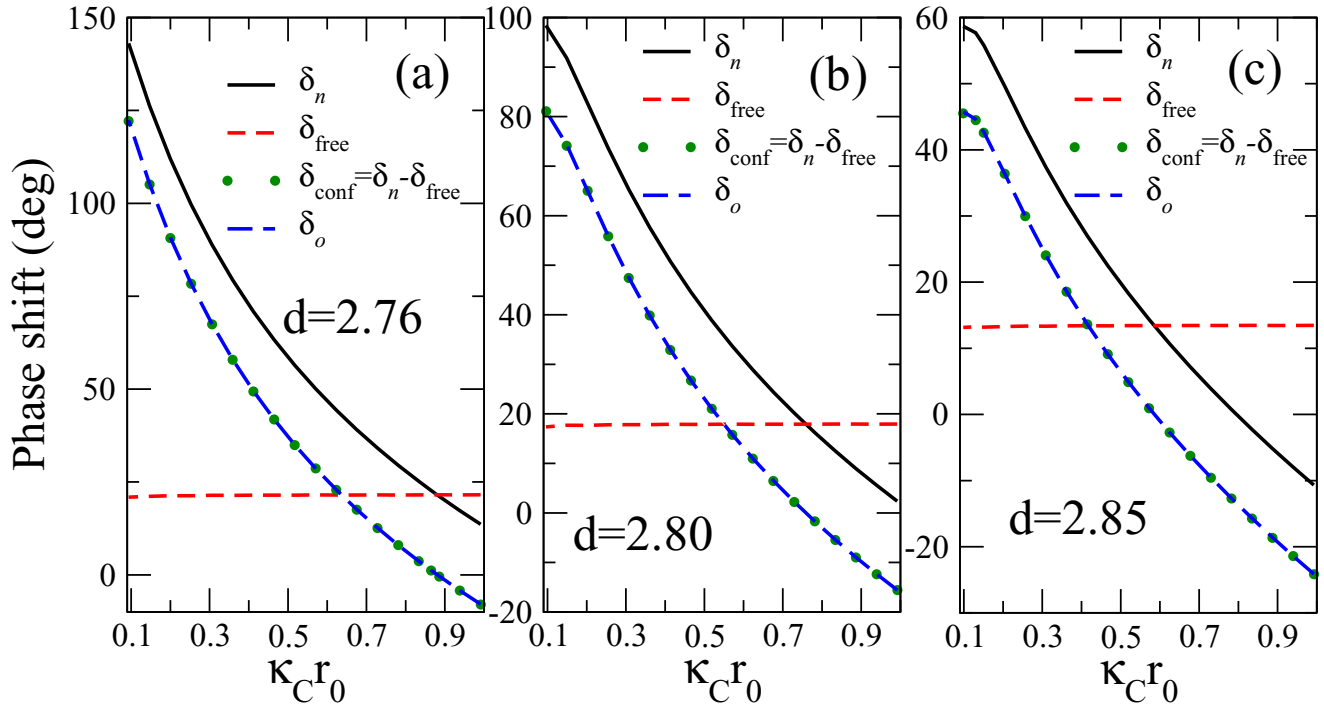
FIG. 4. For the Gaussian potential used in this paper, and three different values of d ($d > d_E$), we give, as a function of $\kappa_C r_0$, the phase shifts δ_n (solid black), δ_{free} (dashed red), δ_{conf} (dotted green), and δ_o (long-dashed blue), obtained after full three-body calculations.

involving simply the projectile and the bound dimer. As a consequence, we can express the low-energy elastic s-wave cross section, σ, for this kind of processes as

$$\sigma_{1+2 \to 1+2} = \frac{4\pi}{\kappa_C^2} \frac{m}{\mu} \sin^2 \delta_o, \qquad (38)$$

where the factor m/μ enters due to the fact that κ_C in Eq. (11) is defined in terms of the normalization mass m, whereas in two-body reactions the correct definition of the momentum should be in terms of the reduced mass, μ, of the projectile-target system. Note that, in this way, Eq. (38) is, as it should be, independent of the arbitrary choice of the normalization mass.

For $1 + 2 \to 1 + 2$ reactions and collision energies below the breakup threshold (or the lowest two-body excitation energy), it is strictly correct that only the lowest adiabatic channel is open. Inclusion of just this open channel provides in general a good approximation, although one or more closed channels may be necessary to get very precise results [36,37]. In such cases the low-energy cross section is well approximated by Eq. (38) [31]. For energies above the breakup threshold, additional (breakup) channels, in principle infinitely many, are also open, and the phase shift corresponding to the elastic channel could be significantly affected by the now open breakup channels. However, for energies still sufficiently close to the breakup threshold, although above, the inelasticity parameter of the collision (which measures the weight of the elastic channel) can still be pretty close to 1, and the cross section in Eq. (38) can still be a good approximation [34].

In the low-energy limit, and close to the Efimov region (large scattering lengths), the phase shift δ_o is given in Eq. (24) after insertion of the appropriate of the two C_2

expressions, which for $1 + 2 \to 1 + 2$ reactions is Eq. (27). Since $\sin^2 \delta_o \approx \delta_o^2 \propto (\kappa_C |a_{\text{av}}|)^{4\ell_C + 2}$, the threshold behavior of the cross section is $\sigma \propto a_{\text{av}}^2 (\kappa_C |a_{\text{av}}|)^{4\ell_C}$. The two-body scattering length then appears to be the unit scale and the approach to zero energy corresponds to scattering for a finite angular momentum, ℓ_C.

C. The $3 \to 3$ reactions

The computed phase shifts, δ_{conf}, in the confined three-dimensional space are given by Eq. (37), which for two-body processes have been found to be the same as the phase shifts obtained in the d formalism. It is interesting to note that this equality, $\delta_{\text{conf}} = \delta_o$, still holds for pure three-body processes, like $3 \to 3$ reactions.

As an illustration we show in Fig. 4, as a function of $\kappa_C r_0$, the values of δ_n (black solid), δ_{free} (red dashed), and δ_{conf} (green dots), for three different dimensions in the $d > d_E$ region, $d = 2.76$ (a), $d = 2.80$ (b), and $d = 2.85$ (c). These phase shifts have been obtained fully numerically from a three-body calculation with the Gaussian potential, as described for the brown dots when discussing Fig. 3. The phase shifts δ_n and δ_{free} are obtained from Eqs. (35) and (36) with and without interaction between the particles, respectively. As mentioned, for these numerical calculations it is not simple to reach $\kappa_C r_0$ values much smaller than about 0.1.

In all the three cases shown in the figure, the trend of the phase shifts is similar, and also, in all the three cases the curve corresponding to δ_{conf} (green dots) perfectly overlaps with the one showing the phase shifts, δ_o, obtained in the d formalism (blue long-dashed). The results shown in the figure have been obtained using the first term, $n = 1$, in the expansion in Eq. (34), which corresponds to $K = 0$ in Eq. (36). We have

checked that the value of δ_{conf} is independent of n, and of course, the result $\delta_{\text{conf}} = \delta_o$ holds no matter the n term used for the calculation.

Therefore, for $3 \rightarrow 3$ reactions, the phase shifts obtained with the d method can also be directly used in the expressions for the cross sections. In particular, considering only the lowest adiabatic elastic channel, the s-wave cross section takes the form [31]

$$\sigma_{3 \rightarrow 3} = \frac{128\pi^2}{\kappa_C^5} \sin^2 \delta_o, \tag{39}$$

where, again, for low energies and large two-body scattering lengths, Eq. (24) can be employed.

The cross section above presents the deficiency of actually depending on the choice made for the normalization mass, m, which is contained in κ_C, as shown in Eq. (11). This is related to the fact that the incoming flux of particles is not well defined when two incident momenta are involved. In order to avoid this problem, it is common for this kind of reactions to deal, not with cross sections, but with reaction rates, which are well defined. In particular, as shown in Ref. [31], the s-wave reaction rate for $3 \rightarrow 3$ processes is given by

$$R_{3 \rightarrow 3} = \frac{32\pi^2}{E^2} \hbar^5 \left(\frac{m_1 + m_2 + m_3}{m_1 m_2 m_3} \right)^{\frac{3}{2}} \sin^2 \delta_o. \tag{40}$$

It is important to keep in mind that for $3 \rightarrow 3$ processes, and even for very low collision energies close to zero, it is not very realistic to assume only one open channel. The other channels related to the other adiabatic three-body potentials may also contribute substantially to these cross sections [31]. This is accentuated close to the Efimov threshold, where a number of bound three-body states are present with extremely small binding energies. All these channels are then open, allowing coupling to related inelastic scattering. To distinguish these processes must be extremely difficult in experiments. In the present theoretical formulation this scattering problem would also be tremendous, but it could perhaps inspire researchers to perform the proper average accessible to experimental tests. Therefore, the expression in Eq. (39), or in Eq. (40), should be taken as a very first approximation to the correct cross section, or reaction rate.

V. SUMMARY AND CONCLUSIONS

In this paper, we use the d method to study three short-range interacting particles in the continuum in a deformed external potential. The d formulation using one decoupled potential in the hyperspherical adiabatic expansion leads to a radial Schrödinger-like equation formally identical to one of two particles. The hyper-radius is the crucial distance coordinate describing the average distance between three particles. They may start being infinitely far apart, then moving together, and, after interacting, again moving away from each other. This is either the 3 to 3 scattering or an elastic-scattering process of $1 + 2$ to $1 + 2$, where 2 means that two of the three particles are in a bound state. The formalism and technique are the same for two particles as well as for both these cases, but the potentials differ from each other.

We insist on applications including the particularly interesting phenomenon known as the Efimov effect. With this in mind, we construct an analytically solvable three-body model, where the key quantity is the effective three-body potential. The details of the short-distance properties are unimportant, and we could as well use a zero-range potential. More precisely, we use a square well in ρ space with a very short radius leaving the square-well parameter to be adjusted to produce the Borromean region of a more realistic potential.

The intermediate region extends from the square-well radius to the two-body scattering length for identical bosons, or to a specified average of two-body scattering lengths for nonequal particles. When the scattering lengths are sufficiently large, the shape and strength of the effective three-body potential in this region are dictated by the large-distance (but still smaller than the scattering length) asymptotic centrifugal barrier structure, which can be obtained from a transcendental equation without any knowledge of the potentials. This amounts to use of a generalized complex angular momentum. This potential can also be found from Gaussian two-body potentials, and then of a different, but similar, structure which requires numerical solution.

The last coordinate interval is beyond the two-body scattering length. The d-dependent angular momentum barrier remains for d values larger than d_E, where the two-body subsystems are unbound. For d smaller than d_E, the large-distance structure of two bound particles is possible and the adiabatic potential can be translated by the corresponding binding energy, still maintaining the formulation.

We calculate analytically the continuum states in this model as well as the related scattering phase shifts, from which the low-energy threshold behavior and cross sections are derived. The generalized d-dependent angular momentum quantum number provides the energy power of the phase shift approach as the energy converges towards zero. We have compared the results obtained from the analytic expressions using the parameters of a Gaussian and a square-well potential that give rise to the same critical dimension, d_E, which provides a pretty similar Borromean region for the three-body system in both cases. The results are to a large extent potential independent when the dimension is close to d_E. Numerical results obtained directly from two-body potentials are virtually impossible to obtain in this dimension region for very small energies, as demanded for instance in $1 + 2 \rightarrow 1 + 2$ elastic reactions, since the energies of the bound two-body states in the region close to the Efimov point are, by definition, extremely small. The analytic results then become the only realistic way of studying these reactions. For sufficiently large energies, where numerical calculations are more accessible, the agreement with the analytic results is remarkable.

The d formulation with spherical potentials is substantially simpler by using a conserved generalized angular momentum quantum number. The external deformed field necessarily involves large numbers of partial waves. However, to compute observable cross sections a translation to the complicated external field formulation in three dimensions is necessary. We have shown numerically that the d-method phase shift is identical to the difference between external field phase shifts with and without short-range interaction. In other words, the

d-method phase shifts are the ones in the confined three-dimensional space, and they are then directly describing the scattering between three particles. In particular the low-energy cross section can be obtained with the analytic expressions for the d-phase shift derived in this paper, and they vanish with a d-dependent power of energy.

In conclusion, we have investigated and illustrated three-body scattering processes in a d-dimensional space, equivalent to a confined three-dimensional space, by use of an analytic schematic model. The cross-section behavior and the insight obtained are universal, that is, independent of details of the employed short-range potentials. The translation from d

to external field is necessary, available, and at least a semiaccurate description. The perspective in our investigations is that scattering between particles confined by deformed external fields may be a useful tool in investigations of for example structures related to Efimov physics. Transitions between other dimensions may also be of interest.

[1] V. Efimov, Phys. Lett. B **33**, 563 (1970).

[2] L. W. Bruch and J. A. Tjon, Phys. Rev. A **19**, 425 (1979).

[3] T. K. Lim and B. Shimer, Z. Phys. A **297**, 185 (1980).

[4] E. Nielsen, D. V. Fedorov, and A. S. Jensen, Phys. Rev. A **56**, 3287 (1997).

[5] A. G. Volosniev, D. V. Fedorov, A. S. Jensen, and N. T. Zinner, Eur. Phys. J. D **67**, 95 (2013).

[6] P. Naidon and S. Endo, Rep. Prog. Phys. **80**, 056001 (2017).

[7] E. Nielsen, D. V. Fedorov, A. S. Jensen, and E. Garrido, Phys. Rep. **347**, 373 (2001).

[8] J. Levinsen, P. Massignan, and M. M. Parish, Phys. Rev. X **4**, 031020 (2014).

[9] M. T. Yamashita, F. F. Bellotti, T. Frederico, D. V. Fedorov, A. S. Jensen, and N. T. Zinner, J. Phys. B **48**, 025302 (2015).

[10] J. H. Sandoval, F. F. Bellotti, A. S. Jensen, and M. T. Yamashita, J. Phys. B **51**, 065004 (2018).

[11] D. S. Rosa, T. Frederico, G. Krein, and M. T. Yamashita, Phys. Rev. A **97**, 050701(R) (2018).

[12] E. R. Christensen, A. S. Jensen, and E. Garrido, Few-Body Syst. **59**, 136 (2018).

[13] E. Garrido, A. S. Jensen, and R. Álvarez-Rodríguez, Phys. Lett. A **383**, 2021 (2019).

[14] E. Garrido and A. S. Jensen, Phys. Rev. Res. **1**, 023009 (2019).

[15] E. Garrido and A. S. Jensen, Phys. Rev. Res. **2**, 033261 (2020).

[16] E. Garrido and A. S. Jensen, Phys. Lett. A **385**, 126982 (2021).

[17] E. R. Christensen, E. Garrido, and A. S. Jensen, Phys. Rev. A **105**, 033308 (2022).

[18] J. M. Vogels, C. C. Tsai, R. S. Freeland, S. J. J. M. F. Kokkelmans, B. J. Verhaar, and D. J. Heinzen, Phys. Rev. A **56**, R1067(R) (1997).

[19] Ph. Courteille, R. S. Freeland, D. J. Heinzen, F. A. vanAbeelen and B. J. Verhaar, Phys. Rev. Lett. **81**, 69 (1998).

[20] E. Nielsen, D. V. Fedorov, and A. S. Jensen, Phys. Rev. Lett. **82**, 2844 (1999).

[21] T. Köhler, K. Góral, and P. S. Julienne, Rev. Mod. Phys. **78**, 1311 (2006).

[22] I. Bloch, J. Dalibard, and W. Zwerger, Rev. Mod. Phys. **80**, 885 (2008).

[23] C. Chin, R. Grimm, P. Julienne, and E. Tiesinga, Rev. Mod. Phys. **82**, 1225 (2010).

[24] S. Deng, Z.-Y. Shi, P. Diao, Q. Yu, H. Zhai, R. Qi, and H. Wu, Science **353**, 371 (2016).

[25] D. Hove, E. Garrido, P. Sarriguren, D. V. Fedorov, H. O. U. Fynbo, A. S. Jensen, and N. T. Zinner, J. Phys. G **45**, 073001 (2018).

[26] B. Simon, Ann. Phys. (NY) **97**, 279 (1976).

[27] L. D. Landau, and E. M. Lifshitz, in *Quantum Mechanics: Non-Relativistic Theory* (Pergamon Press, New York, 1977), p. 163.

[28] A. S. Jensen, K. Riisager, D. V. Fedorov, and E. Garrido, Rev. Mod. Phys. **76**, 215 (2004).

[29] T. Frederico, A. Delfino, L. Tomio, and M. T. Yamashita, Prog. Part. Nucl. Phys. **67**, 939 (2012).

[30] N. T. Zinner and A. S. Jensen, J. Phys. G **40**, 053101 (2013).

[31] E. Garrido, Few-Body Syst. **59**, 17 (2018).

[32] A. Messiah, *Quantum Mechanics* (North-Holland, Amsterdam, 1961), Vol. 1, p. 385.

[33] M. A. Shalchi, M. T. Yamashita, M. R. Hadizadeh, E. Garrido, Lauro Tomio, and T. Frederico, Phys. Rev. A **97**, 012701 (2018).

[34] E. Garrido, C. Romero-Redondo, A. Kievsky, and M. Viviani, Phys. Rev. A **86**, 052709 (2012).

[35] E. Garrido, M. Gattobigio, and A. Kievsky, Phys. Rev. A **88**, 032701 (2013).

[36] P. Barletta, C. Romero-Redondo, A. Kievsky, M. Viviani, and E. Garrido, Phys. Rev. Lett **103**, 090402 (2009).

[37] C. Romero-Redondo, E. Garrido, P. Barletta, A. Kievsky, and M. Viviani, Phys. Rev. A **83**, 022705 (2011).

[38] J. P. D'Incao and B. D. Esry, Phys. Rev. Lett. **94**, 213201 (2005).

[39] T. Regge, Nuovo Cimento **14**, 619 (1959).

[40] D. V. Fedorov and A. S. Jensen, Europhys. Lett. **62**, 336 (2003).

[41] M. Mikkelsen, A. S. Jensen, D. V. Fedorov, and N. T. Zinner, J. Phys. B **48**, 085301 (2015).

[42] V. Efimov, Nucl. Phys. A **210**, 157 (1973).

[43] P. Naidon, S. Endo, and M. Ueda, Phys. Rev. A **90**, 022106 (2014).

[44] E. Garrido and A. S. Jensen, Few-Body Syst. **62**, 25 (2021).

[45] P. Naidon, S. Endo, and M. Ueda, Phys. Rev. Lett. **112**, 105301 (2014).